Soft Matter

COMMUNICATION

View Article Online
View Journal | View Issue

Cite this: *Soft Matter*, 2017, 13, 2903

Received 3rd March 2017,
Accepted 24th March 2017

DOI: 10.1039/c7sm00446j

rsc.li/soft-matter-journal

Photo-induced structural modification of silk gels containing azobenzene side groups†

Michael J. Landry,[a] Matthew B. Applegate,[b] Oleksandr S. Bushuyev,[a] Fiorenzo G. Omenetto,[b] David L. Kaplan,[b] Mark Cronin-Golomb *[ab] and Christopher J. Barrett *[a]

Azobenzene modification of *Bombyx mori* silkworm silk creates a photo-responsive 'azosilk' biomaterial, allowing for 3D laser patterning. Written regions fluoresce, and become fluid-filled raised 'micro-blisters' with a 10-fold photo-softening effect of the modulus. Patterning is facile and versatile, with potential applications as soft tunable materials for dynamic cell guidance and microfluidics.

Silk fibroin from *Bombyx mori* silkworms is a versatile biocompatible material receiving recent interest in tissue engineering, bioelectronics and optics.[1–4] The optical clarity of silk films and gels make it attractive for applications in the design of some biomedical devices, particularly implantable optical components requiring soft biocompatible parts.[5–8] Many of these applications require the ability to pattern the material and thus several methods have been reported including soft lithography,[9,10] nano-imprinting,[11,12] electron lithography,[13,14] chemical modification of silk to form methacrylate-based photoresists,[15] and optical micromachining in cross-linked silk hydrogels.[16]

When silk is processed into useful materials such as films, microspheres, sponges, tubes, gels and fibers, it can retain the elastic properties related its secondary structure. Silk possesses regions of highly repetitive sequences of amino acids, which lead to well-defined structural domains. This offers the potential for facile and controllable chemical modifications with photo-active compounds, to introduce the ability to post-engineer its physical properties using light. A convenient method for this is to use diazonium coupling to the tyrosine residues, effectively incorporating light-responsive azobenzene into the silk structure. Azobenzene and its derivatives see wide use in developing optically sensitive materials for applications including optical storage, holography,[17,18] and optically actuated micro-mechanical systems (MEMS),[19–21] based on reversible photo-switching between the *trans* and *cis* geometric isomers. The recent demonstration of the functionalization of silk with various azobenzene moieties (azosilk) provides a facile route to incorporate the optical properties of azobenzene into silk.[22,23]

Azosilk has previously been shown to exhibit optically-induced birefringence and holographic recording in dry thin films.[23] In this paper, we report the discovery that permanent three-dimensional topographic micro-patterning in hydrated azosilk films can be achieved through photo-induced physical modification of azosilk films using the photolithographic capabilities of a nonlinear scanning microscope. We observed two newly discovered light-induced changes: a significant shift in fluorescence emission wavelength, and key to proposed applications: volume morphology changes, which subsequently control surface stiffness over a wide range. The morphology changes are in the form of raised blisters, which have the potential to guide cells through modulus and topography changes on the surface of the silk films.

We prepared azosilk materials following previous literature protocols,[22] with some modifications (see ESI†) and cast them into thin films. Films were submerged into water to ensure even hydration and a dipping lens was used to minimize scattering during the writing. The water content of these films was found to comprise 77 wt% of the material from TGA characterization (Fig. S4, ESI†). While studying the optical properties of these azosilk films with a nonlinear scanning microscope using a femtosecond mode-locked laser at 800 nm, we observed that the regions under observation fluoresced with peak emission at 625 nm corresponding to the known fluorescence of azobenzene,[24] but over time developed significantly increased fluorescence accompanied by a shift of the emission peak to 520 nm (Fig. S1, ESI†). Desired areas could be patterned using a Zeiss Axioexaminer nonlinear optical scanning microscope, with specific regions of interest exposed to laser light to form precise and arbitrary composite patterns.[25] This lithographic technique allows for the creation of complex patterns by combining numerous programmable exposure areas referred to in the software as 'regions of interest'. These regions are generated by a Matlab code[25] from a black and white image,

[a] *Department of Chemistry, McGill University, 801 Sherbrooke Street West, Montreal H3A 0B8, Canada. E-mail: christopher.barrett@mcgill.ca*
[b] *Department of Biomedical Engineering, Tufts University, 4 Colby Street, Medford 02155, USA. E-mail: mark.cronin-golomb@tufts.edu*

† Electronic supplementary information (ESI) available. See DOI: 10.1039/c7sm00446j

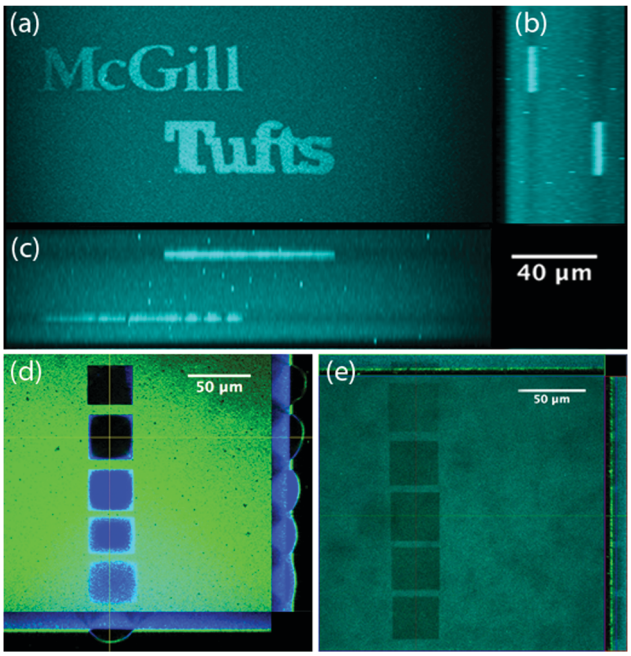

Fig. 1 (a) Written areas of the hydrated azosilk film show increased fluorescence compared to the unwritten areas at two different depths within the hydrated film. The darkening shown in the writing planes is an artifact of the software. (b) Vertical projection of three-dimensional photolithography image of (a). (c) Horizontal projection of the image shown in (a). (d) Confocal fluorescence image at 488 nm excitation (blue) and reflectance image (green) of hydrated azosilk with photo-modified regions. From top to bottom, each rectangle is written 1 μm deeper into the azosilk. The cross-sections of the film show the development of blisters whose thickness decreases with writing depth. Each 37 μm × 37 μm rectangle takes 1.5 seconds of writing time. Each 0.4 μm × 0.4 μm pixel receives 2500 pulses each with 1.25 nJ energy and 250 fs pulse width. (e) Confocal fluorescence imaging at 488 nm excitation (blue) and reflectance image (green) of hydrated unmodified silk pattern-irradiated in the same manner as (a), showing lack of blistering.

thus allowing for the programmable patterning of complex and arbitrary written areas within the film. Fig. 1a–c presents an example where such spatial control over laser irradiation enables the inscription of the test words ''McGill'' and ''Tufts'' at different depths in the film composed of more than 200 regions of interest. The fluorescent patterns were formed using two-photon femtosecond pulse excitation at 800 nm at 80 MHz repetition rate within these regions of interest. The width of the pulses was 250 fs after including the dispersive effects of the objective lens and the acousto-optic modulator in the microscope after the laser (Chameleon by Coherent). The fluorescence patterns that result represent a facile marker of visually tracking the inscribed areas. When the writing energy was increased to 100 μJ μm^{-2} (2500 pulses), a more important physical effect was observed; the film would form large soft raised blisters on the surface of the material, coincident with the lithographic irradiation pattern. These blisters were filled with a fluorescent liquid whose peak emission wavelengths closely matched those of plain silk photo-irradiated by more intense 800 nm light (900 μJ μm^{-2}).

To study the blister formation, a set of 5 rectangles was written (Fig. 1d). The rectangle at the top of the figure was written just under the surface, and subsequent rectangles presented below it were written at increasing depth in the film in steps of 1 μm. While the axial resolution of the microscope under the conditions used is only about 1 μm, the peak intensity of the beam can still be stepped in down in 1 μm increments, with corresponding shifts in the mean depth of illumination and pattern writing. Within Fig. 1d and e, green colour indicates the surface of the film by reflectance confocal while blue corresponds to broadband fluorescence excited at 488 nm, showing signals from the unexposed azosilk as well as fluorescence from the exposed areas. The film expands vertically (parallel to the axis of the laser beam) to form blisters with the height of 13 μm for samples irradiated near surface. The blister height decreases upon an increase in writing depth presumably because stronger physical confinement deep in the hydrated film. The uniformity of fluorescence in the material within the blisters suggests that they are liquid-filled. The top two bubbles appeared to be so thin that their porosity allowed the fluorescent contents to escape into the surrounding water solution, while the lower three blisters remained intact and fluid-filled.

To determine the contents of the fluid-filled blisters, a series of 100 disc shaped blisters were created and their liquid was manually extracted using a micro-needle. NMR analysis was conducted on the withdrawn liquid and it was concluded that the fluorescent liquid was mainly water along with some trace amino acid residues (see ESI†). Fluorescence lithography was also performed in hydrated unmodified silk as a control, with very different results observed at the same writing parameters than for azosilk (Fig. 1e). In this case, fluorescence peaking at 470 nm is simply diminished in intensity, and no blistering is observed. When the writing energy is increased to 900 μJ μm^{-2}, the plain silk films sustain observable structural damage that does not conform closely to the lithography pattern (Fig. S3, ESI†). There is a simultaneous increase in fluorescence intensity in the damaged regions accompanied by a 20 nm shift towards shorter wavelengths. Irradiation of hydrated films of azosilk produces permanent fluorescent blisters written into them, with patterns still easily observable after 3 months as long as they are kept under water. The fluorescence spectra (Fig. S1, ESI†) of written and unwritten regions in various samples were recorded using the microscope's emission spectroscopy mode with two-photon excitation at 800 nm. Unmodified silk shows an emission spectrum peaking at 470–500 nm, unwritten azosilk shows a fluorescence peak at 640 nm, while written azosilk shows fluorescence at 520 nm and 560 nm.

While there have been previous observations of fluorescence in azobenzene and azobenzene-containing polymers,[24,26] the observed fluorescence in azosilk appears to be closely analogous to that obtained in experiments with silk treated with horseradish peroxidase (HRP).[27] HRP has been shown previously to convert unmodified silk solutions into a fluorescent hydrogel with dityrosine crosslinks.[27,28] However, in the case of azosilk, the azobenzene pendant groups on the tyrosine residues extend the pi-system and lead to a broader fluorescence signal. We hypothesize that the optically-induced modifications observed in azosilk are due to the two-photon absorption of the azobenzene

in the azosilk, and reaction of the resulting photo-excited radicals on tyrosine moieties to form dityrosine, leading to disruption of the self-assembled structure, then expansion and blistering. This is consistent with the fluorescence effects observed in HRP crosslinked silk where the HRP produces dityrosine bonds and results in enhanced blue fluorescence.[27]

To test the hypothesis that photo-induced fluorescence changes are due to photo-crosslinking of radical species, the radical marker TEMPO ((2,2,6,6-tetramethylpiperidin-1-yl)oxyl) was added to hydrated films. At high concentrations of TEMPO (10 wt%), writing into the film was not observed but could be re-established by washing out the TEMPO from within the film with a 50 : 50 water : ethanol solution. This may be due to TEMPO competing for the radicals that would otherwise be used by the excited tyrosine when crosslinking into dityrosine. Fluorescence modification is re-established with decreasing TEMPO concentrations. When the concentration of the added TEMPO drops below 1 wt%, fluorescence modification is induced; however, blistering is not observed regardless of irradiation power. At higher concentrations of TEMPO (5–10 wt%), fluorescence decreases upon illumination by the mode-locked laser. Writing was not observed within an azosilk sample prepared with 10% TEMPO at any power. To confirm the role of water during blister formation, films were exposed to 800 nm irradiation under dry conditions (Fig. S5, ESI†). Written areas in dry films exhibit the same fluorescence shift as seen for hydrated azosilk films (Fig. S6, ESI†), but no blistering occurs. This supports our hypothesis that water is required for the blistering to occur, and allows us to separate the two effects of the fluorescence shifts and the blistering.

AFM force imaging (Fig. 2, Asylum Research MFP-3D) showed that the modulus of the azosilk in unwritten areas was 12 ± 1 kPa. This decreased to 0.6 kPa in the photo-modified areas and the measurement was replicated in many different areas to ensure consistency. To our knowledge, controlled photo-softening of this magnitude has not previously been observed in any silk material. This is an interesting feature for potential cell-guidance control applications, as variations in modulus have been shown to exert influence over various cell processes and functions, including growth orientation of neural cells.[29–31] One could easily envisage that this softening effect could be controlled to vary predictably with writing depth from the surface, in addition to the power and duration of irradiation, to tune this photo-softening in the patterns.

In summary, we have found that the azobenzene in azosilk can act as a photo-sensitizer that produces a photolithographic material exhibiting a new physical 'soft blistering' effect previously unreported or explored in any azopolymers. It enables visible light to be used in a precise and localized manner to inscribe programmable patterns and morphologies on silk biomaterials in a single post-processing step. There are several potential applications for such photo-induced blisters that could readily be envisaged in addition to cell influence, for example this effect might be used to form microfluidic channels in the same way that multi-photon absorption can be used to form channels in horseradish peroxidase (HRP) crosslinked silk.[16] As an illustration of this potential application, we wrote a microfluidic test pattern[32] in azosilk (Fig. 3) based on a standard test device design. The image of the pattern was recorded with an ordinary wide field microscope, indicating that patterns can

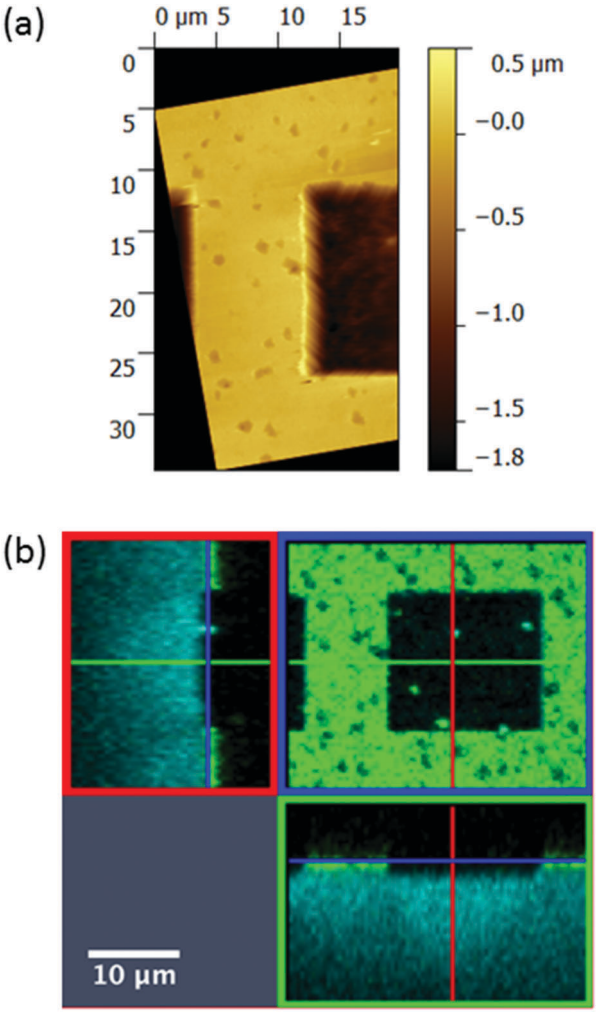

Fig. 2 (a) AFM image of photo-inscribed areas of azosilk (b) the corresponding confocal image. Blue channel: fluorescence at 488 nm excitation. Green channel: reflectance image. The blister top has completely separated from surface in this case.

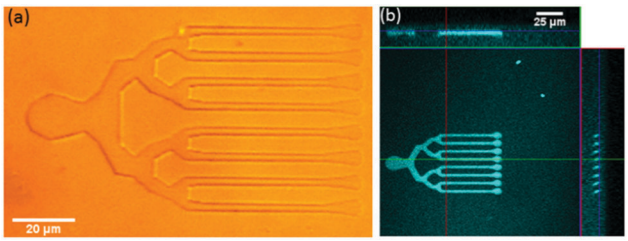

Fig. 3 (a) Wide field image of a microfluidic-inspired pattern made through the ocular of the microscope, demonstrating that the photo-inscribed structures can be easily visualized with an ordinary wide field microscope, so they can be readily found for later processing. (b) Cross sectional image of a microfluidic pattern written within the hydrated azosilk film showing the increased fluorescence obtained by irradiating several regions of interest.

be easily observed using conventional microscopy. In this case, the size of the microfluidic chamber would be limited by the field of view of the objective used on the microscope being used for lithography, unless indexed and moved, but otherwise unlimited in 2D patterns possible and so represents a facile method to fabricate microfluidic chambers without the use of expensive photo-resist masks and clean room procedures.

Conclusions

In conclusion, photo-induced patterning in azosilk materials provides optically tunable surfaces and topologies generated by laser light irradiation. These photo-inscribed regions also show a controlled decreased modulus, illustrating a tunable photo-softening effect. This patterning of azosilk films can be readily accomplished through a one-step two-photon process, and provides promising surfaces for a wide variety of potential applications such as microfluidic inscription, dynamic directed cell-growth surfaces, and in general as localized optically-modifiable soft biomaterials.

Acknowledgements

Images were collected, processed, and analyzed for this manuscript in the McGill University Life Sciences Complex Advanced BioImaging Facility (ABIF). We thank the AFOSR (Tufts) and NSERC Canada (McGill) for support of this work. CJB and MCG are grateful for funding from FQRNT Quebec Canada, which assisted a sabbatical stay at McGill University's Centre for Self-Assembled Chemical Structures. CJB is grateful to the Artisans d'Angkor and Kolbe Foundations for enabling a visit to *Bombyx Mori* silkworm farms and silk harvesting facilities in Cambodia, with in-kind supply of silk cocoons.

Notes and references

1 Z.-H. H. Li, S.-C. C. Ji, Y.-Z. Z. Wang, X.-C. C. Shen and H. Liang, *Front. Mater. Sci.*, 2013, **7**, 237–247.
2 A. U. Ude, R. A. Eshkoor, R. Zulkifili, A. K. Ariffin, A. W. Dzuraidah and C. H. Azhari, *Mater. Des.*, 2014, **57**, 298–305.
3 S. Van Vlierberghe, P. Dubruel and E. Schacht, *Biomacromolecules*, 2011, **12**, 1387–1408.
4 F. G. Omenetto and D. L. Kaplan, *Science*, 2010, **329**, 528–531.
5 L. J. Bray, K. A. George, S. L. Ainscough, D. W. Hutmacher, T. V. Chirila and D. G. Harkin, *Biomaterials*, 2011, **32**, 5086–5091.
6 P. C. Demuth, Y. Min, D. J. Irvine and P. T. Hammond, *Adv. Healthcare Mater.*, 2014, **3**, 47–58.
7 J. R. Mauney, G. M. Cannon, M. L. Lovett, E. M. Gong, D. Di Vizio, P. Gomez, D. L. Kaplan, R. M. Adam and C. R. Estrada, *Biomaterials*, 2011, **32**, 808–818.
8 L. Bai, L. Zhu, S. Min, L. Liu, Y. Cai and J. Yao, *Appl. Surf. Sci.*, 2008, **254**, 2988–2995.
9 F. Galeotti, A. Andicsova, S. Yunus and C. Botta, *Soft Matter*, 2012, **8**, 4815.
10 K. Sakakibara, J. P. Hill and K. Ariga, *Small*, 2011, **7**, 1288–1308.
11 G. Ding, Q. Jin, Q. Chen, Z. Hu and J. Liu, *Nanoscale Res. Lett.*, 2015, **10**, 491.
12 H. Perry, A. Gopinath, D. L. Kaplan, L. Dal Negro and F. G. Omenetto, *Adv. Mater.*, 2008, **20**, 3070–3072.
13 S. Kim, B. Marelli, M. A. Brenckle, A. N. Mitropoulos, E. S. Gil, K. Tsioris, H. Tao, D. L. Kaplan and F. G. Omenetto, *Nat. Nanotechnol.*, 2014, **9**, 306–310.
14 J. Liu, J. Shao and J. Zheng, *J. Appl. Polym. Sci.*, 2004, **91**, 2028–2034.
15 N. E. Kurland, T. Dey, S. C. Kundu and V. K. Yadavalli, *Adv. Mater.*, 2013, **25**, 6207–6212.
16 M. B. Applegate, J. Coburn, B. P. Partlow, J. E. Moreau, J. P. Mondia, B. Marelli, D. L. Kaplan and F. G. Omenetto, *Proc. Natl. Acad. Sci. U. S. A.*, 2015, **112**, 12052–12057.
17 H. Audorff, K. Kreger, R. Walker, D. Haarer, L. Kador and H.-W. Schmidt, in *Complex Macromolecular Systems II*, ed. A. H. E. Müller and H.-W. Schmidt, Springer Berlin Heidelberg, Berlin, Heidelberg, 2010, pp. 59–121.
18 A. Shishido, *Polym. J.*, 2010, **42**, 525–533.
19 X. Ye and M. G. Kuzyk, *Opt. Commun.*, 2014, **312**, 210–215.
20 A. Priimagi, C. J. Barrett and A. Shishido, *J. Mater. Chem. C*, 2014, **2**, 7155–7162.
21 I. Krasnov, N. R. Krekiehn, C. Krywka, U. Jung, A. U. Zillohu, T. Strunskus, M. Elbahri, O. M. Magnussen and M. Müller, *Appl. Phys. Lett.*, 2015, **106**, 3702–3706.
22 A. R. Murphy, P. St John, D. L. Kaplan, P. S. John and D. L. Kaplan, *Biomaterials*, 2008, **29**, 2829–2838.
23 M. Cronin-Golomb, A. R. Murphy, J. P. Mondia, D. L. Kaplan and F. G. Omenetto, *J. Polym. Sci., Part B: Polym. Phys.*, 2012, **50**, 257–262.
24 H. Satzger, S. Sporlein, C. Root, J. Wachtveitl, W. Zinth and P. Gilch, *Chem. Phys. Lett.*, 2003, **372**, 216–223.
25 J. C. Culver, J. C. Hoffmann, R. A. Poche, J. H. Slater, J. L. West, M. E. Dickinson, R. A. Poché, J. H. Slater, J. L. West and M. E. Dickinson, *Adv. Mater.*, 2012, **24**, 2344–2348.
26 R. Y. Zhao, X. P. Zhan, J. Yao, G. N. Sun, Q. D. Chen, Z. Q. Xie and Y. G. Ma, *Polym. Chem.*, 2013, **4**, 5382–5386.
27 B. P. Partlow, C. W. Hanna, J. Rnjak-Kovacina, J. E. Moreau, M. B. Applegate, K. A. Burke, B. Marelli, A. N. Mitropoulos, F. G. Omenetto and D. L. Kaplan, *Adv. Funct. Mater.*, 2014, **24**, 4615–4624.
28 G. S. Harms, S. W. Pauls, J. F. Hedstrom and C. K. Johnson, *J. Fluoresc.*, 1997, **7**, 283–292.
29 C. Tomba and C. Villard, *Microelectron. Eng.*, 2015, **132**, 176–191.
30 P. C. Georges, W. J. Miller, D. F. Meaney, E. S. Sawyer and P. A. Janmey, *Biophys. J.*, 2006, **90**, 3012–3018.
31 P. C. Georges and P. A. Janmey, *J. Appl. Physiol.*, 2005, **98**, 1547–1553.
32 E. W. K. Young, A. R. Wheeler and C. A. Simmons, *Lab Chip*, 2007, **7**, 1759–1766.

